

Further observations of Capella in the He I $\lambda 10830 \text{ \AA}$ line: the activity cycle and role of binarity effects

M.M. Katsova¹ and A.G. Shcherbakov²

¹ Sternberg State Astronomical Institute, Moscow State University, 119899 Moscow, Russia (e-mail: maria@sai.msu.su)

² Crimean Astrophysical Observatory, 334413 Nauchny, Crimea (e-mail: sherb@crao.crimea.ua)

Received 6 December 1996 / Accepted 29 August 1997

Abstract. High dispersion CCD spectra of the spectroscopic binary Capella in the infrared He I $\lambda 10830 \text{ \AA}$ line were obtained with the Shajn 2.6-m telescope of the Crimean Astrophysical Observatory during 1989–1994 over several orbital periods. An analysis of new data confirms our earlier conclusions: i) the main (narrow) He I $\lambda 10830 \text{ \AA}$ line is formed in the outer atmosphere of the primary, cooler component, which is a G6 giant, as follows from the dependence of the radial velocity curves of the He I and photospheric lines on the orbital period; and ii) the equivalent width of the He I line varies with the 104-day orbital period of Capella’s binary. The mean level of the equivalent width values changes from year to year.

We show that the amplitude of variations of the equivalent width as a function of the orbital phase becomes lower when the mean level of the equivalent width is higher. The long-term variability of the helium absorption is reliably determined from uniform CCD observations in 1985–1994; this variability is associated with an activity cycle with a period of 6 years (this cycle is traced through the whole set of our data since 1980). During a season when the activity level of the Capella system was high, we were able for the first time to identify the fraction of the He I absorption formed in the chromosphere of the active, hotter F9 giant.

All these helium data together with the EUV results of Dupree & Brickhouse (1995) on the high-temperature Fe XX–Fe XX III lines can be explained using a model with an enhanced magnetized stellar wind that originates from a local region on the active F9 giant, and then forms a shock wave in the outer layers of the corona of the quiescent G6 giant.

Key words: stars: activity – stars: atmospheres – binaries: spectroscopic – Capella – stars: late-type

1. Introduction

Solar-like activity phenomena occur not only on active late-type dwarf stars, but also on some fast-rotating late-type subgiants and giants. There are several pieces of observational evidence

for activity on the F9 giant in Capella’s binary system. The spectroscopic binary α Aur Aa and Ab in the Capella multiple stellar system is one of the most famous targets for investigations both of activity in the outer atmospheres of late-type stars and of the influence of binarity on activity and stellar evolution. This binary system has an orbital period of 104 days and consists of two giants: a cooler G6 III primary and a hotter F9 III secondary. It has now been verified that the F9 giant secondary has a more active outer atmosphere compared to the primary star, as was supposed for the first time by Katsova & Livshits (1978) and finally established by Ayres & Linsky (1980). Further detailed investigations of Capella’s spectra have been carried out using IUE, HST and EUVE. It should be noted here that final results of a re-analysis of the IUE data for Capella have been given by Wood & Ayres (1995), who showed that a significant part of the UV radiation of Capella is from the transition region of the hotter, F9 giant. According to the HST data (Linsky et al. 1995), the ratio of the UV emission line flux of the F9 star transition region to that of the G6 giant is 1.35 for the C IV line, greater than 1.3 for the Si IV, Si III, C II, and close to 1.15–1.20 for the emission lines of neutral elements such as O and C. The surface fluxes of Capella’s active regions are 10 times higher than those in the quiet outer atmosphere. The corresponding solar ratios are a factor of 2–3 lower; i.e., active regions on Capella are developed more intensively. On the other hand, the modulation of these UV lines, including the C IV doublet, with the period of the axial rotation of the F9 giant (around 8 days) is rather weak, this apparently indicates that the distribution of active regions over the F9 stellar surface is more or less homogeneous. Investigations of such solar-like activity on Capella are of interest; we will consider here, in particular, evidence for the presence of an activity cycle from our homogeneous set of observations.

In addition, we are now apparently encountering active phenomena that have no direct analogues in solar physics. We found this for the first time for Capella during analysis of absorption in the near infrared He I $\lambda 10830 \text{ \AA}$ line, moreover this absorption is located mainly on the quiescent G giant (Shcherbakov et al. 1990).

Capella’s binary can be considered an the RS CVn-type binary systems, but with a long orbital period. We have argued

that some part of the activity in these systems are directly due to the effect of binarity. To interpret some radio, near infrared and X-ray observations during the quiescent state of the RS CVn binaries, and especially during rare flares, we must assume a source with a size an order of magnitude larger than the radius of the active component. Recent observations of Capella with the EUV Explorer by Dupree & Brickhouse (1995) are of great interest for studies of the role of binarity effects in activity phenomena: variations of the Fe XX–Fe XXIII line fluxes with the phase of the 104-day orbital period were found. The effects of binarity on the activity in the He I λ 10830 Å line can be explained in the framework of the physical model proposed earlier by Katsova (1992, 1995).

Here we present and analyze new observations of the He I λ 10830 Å line in Capella during 1989–1994. The first observations of this near infrared He I line in Capella were carried out more than 15 years ago (Zirin 1976; Katsova & Shcherbakov 1983) when both photomultiplier and high-sensitive infrachromatic film were used. Since 1985, we have been using a high dispersion, red-sensitive CCD imaging system installed on the coude spectrograph of the Shajn 2.6-m telescope of the Crimean Astrophysical Observatory. These latter observations show variability of the equivalent width of the He I λ 10830 Å line of Capella associated with activity modulation due to the orbital period (104 days) and probably axial rotation of the F9 giant (8–10 days, Fekel et al., 1986).

We have continued our investigation of the temporal behaviour of the near infrared helium line using observations during 1989–1994. We confirm our previous conclusions about the dependence of the EW(He I) on orbital phase, and also investigate its behaviour through the time interval 1980–1994. In addition to the orbital variations of the EW(He I), we have found long-term variability in the helium absorption, which is reliably determined from uniform CCD observations in 1985–1994. We are also able to separate the contributions of each of stars to the He I λ 10830 Å absorption observed during seasons of high activity in Capella.

2. Observations and data reduction

Observations of Capella were carried out from the winter of 1989 to the spring of 1994 at the Crimean Astrophysical Observatory. High-dispersion spectra of Capella were obtained using the Helsinki Observatory CCD imaging system based on the GEC red-sensitive CCD (Huovelin et al. 1986), and the CCD imaging system of Ista Ltd, St.Petersburg (Beresin et al. 1991). Both systems were installed on the coude spectrograph of the 2.6-m Shajn telescope. The original reciprocal dispersion was 0.12 Å /pixel. To increase the coude spectrograph transparency the entrance slit width was increased to 0.4 for the near infrared He I line observations. This slit width corresponds to spectral resolution of $R = 32\,000$. Depending on the seeing and atmospheric transparency, we achieved signal-to-noise ratios of 100 with Helsinki Observatory system and 25–30 with Ista Ltd system. All spectra obtained at the 2.6-m Shajn telescope under the control of the 3A software package

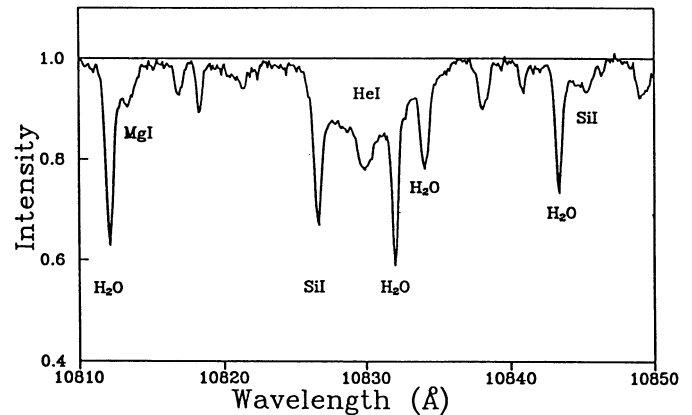


Fig. 1. The spectrum of Capella in the He I λ 10830 Å line at the orbital phase 0.62 on 26.09.1993

(Ilyin 1995) were extracted using CCD-FIT package developed by V.A.Shcherbakov (1994). Flat-field correction and a spike-deleting procedure were carried out before extracting the spectra. The spectra were normalized to the local continuum.

The He I λ 10830 Å absorption line is blended by photospheric absorption in the Si I λ 10827 Å line and two water vapor lines H₂O λ 10832 Å and λ 10834 Å in the Earth's atmosphere. These terrestrial H₂O lines were usually used for the wavelength calibration. After the effect of the Earth's motion was removed, we derived the absolute wavelength scale. Since the He I, Si I and H₂O lines are formed in different physical regions, they can easily be separated. The profiles of the H₂O lines were fitted by Gaussian profiles and then, more accurately (taking into account the water line wings), by Pearson profiles. The Si I line profile was fitted by a Voigt profile using the observed blue wing of the line. These blends were extracted from the observed spectra to measure the equivalent width of the helium line and the radial velocity of the centre of gravity of the profile. We were able to evaluate the equivalent widths of both the He I λ 10830 Å and Si I λ 10827 Å lines for all 90 spectra. About 50 spectra obtained from 1989 to 1994 are of very high quality, and can be used not only to determine radial velocity curves based on several lines of both components, but also to trace time variations of the He I line profile and to separate the contribution of each component to the lines.

3. Results

3.1. Radial velocities

The results of the radial velocity measurements, together with the observational data, phases of the orbital period 104^d.0214 at zero epoch $T_0 = JD2432861.440$ (Shen et al. 1985), and equivalent widths of the He I λ 10830 Å line are presented in Table 1.

A typical near-infrared spectrum of Capella is shown in Fig. 1. Some of the spectra obtained in 1990 and 1993–1994 demonstrate asymmetric He I line profiles, however. We distinguished the He I λ 10830 Å line profile for two components of

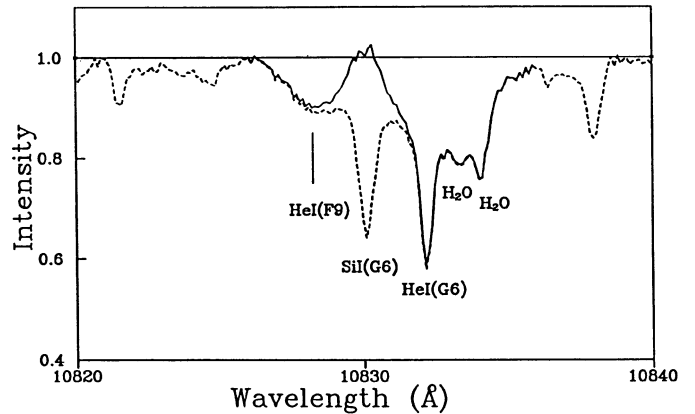
Table 1.

Date	JD 244+	Orbital phase	EW (Å)	RV(G6) km s ⁻¹
1989				
14.12	7874.743	0.329	1.08	22.34
16.12	7876.711	0.348	0.96	18.53
25.12	7885.723	0.434	1.15	6.00
1990				
31.01	7922.512	0.788	0.87	38.23
08.03	7959.492	0.144	0.86	37.60
16.03	7967.386	0.220	1.08	–
17.03	7968.469	0.230	0.91	–
05.04	7987.438	0.412	1.18	12.27
16.08	8119.673	0.684	0.96	24.15
01.09	8135.702	0.838	0.84	40.36
14.11	8209.534	0.547	1.07	10.53
27.11	8222.507	0.672	0.98	22.97
12.12	8238.290	0.824	0.97	–
25.12	8251.319	0.949	0.90	–
25.12	8251.453	0.950	0.79	–
1991				
09.03	8325.317	0.660	0.94	–
03.11	8563.503	0.950	0.59	–
1992				
24.02	8677.464	0.046	0.50	–
11.09	8876.637	0.961	0.86	–
1993				
03.01	8990.554	0.056	0.44	–
03.01	8990.577	0.056	0.53	–
06.01	8993.549	0.085	0.52	–
06.01	8993.594	0.085	0.59	–
07.01	8994.534	0.094	0.64	–
07.01	8994.550	0.094	0.72	–
03.02	9022.333	0.361	0.73	–
03.02	9022.357	0.362	0.75	–
05.02	9024.446	0.382	0.80	–
10.03	9057.414	0.699	0.68	–
10.03	9057.441	0.699	0.74	–
12.03	9059.410	0.718	0.66	–
12.03	9059.434	0.718	0.64	–
16.03	9063.380	0.756	0.65	–
09.09	9239.542	0.449	1.07	11.058
10.09	9240.562	0.459	1.05	10.989
11.09	9241.533	0.469	1.10	6.711
11.09	9241.549	0.469	1.07	7.957
11.09	9241.556	0.469	1.07	7.815
11.09	9241.564	0.469	1.10	7.453
11.09	9241.572	0.469	1.03	8.337
11.09	9241.580	0.469	1.07	7.704

the binary system as follows. First, the Si I λ 10827 Å line profile from the G6 giant was extracted from the total blend by fitting it by a Voigt profile using the PeakFit package developed in Jandel Scientific Corporation. An example of this extraction is presented in Fig. 2. The original spectrum is shown by dashed line; it can be seen that after extracting the Si I line, the He I

Table 1. (continued)

Date	JD 244+	Orbital phase	EW (Å)	RV(G6) km s ⁻¹	RV(F9) km s ⁻¹
1993					
12.09	9242.545	0.478	0.90	17.139	–
13.09	9243.523	0.488	1.03	5.618	–
15.09	9245.503	0.507	0.93	10.654	–
15.09	9246.496	0.516	0.82	7.244	–
16.09	9247.492	0.526	0.97	6.171	–
26.09	9257.399	0.621	0.94	14.713	–
28.09	9259.380	0.640	1.05	17.166	–
02.10	9263.383	0.679	0.83	20.770	54.03
03.10	9264.378	0.688	0.80	21.616	55.56
23.10	9283.514	0.872	0.72	44.828	9.20
24.10	9284.636	0.883	0.78	46.684	7.94
22.11	9314.367	0.169	0.96	35.478	–
23.11	9315.258	0.177	0.95	40.175	–
23.11	9315.281	0.177	0.87	52.717	–
24.11	9316.458	0.189	0.87	22.727	24.50
24.11	9316.480	0.189	0.82	22.668	24.05
28.11	9320.473	0.227	0.91	27.396	27.77
28.11	9320.490	0.228	0.90	28.296	28.09
1994					
21.02	9405.438	0.044	0.81	55.835	2.97
21.02	9405.450	0.044	0.71	57.015	6.37
27.02	9411.439	0.102	0.77	50.257	9.04
27.02	9411.456	0.102	0.72	49.971	9.42
28.02	9412.440	0.111	0.83	48.094	10.30
28.02	9412.450	0.112	0.79	48.690	8.32
25.03	9437.258	0.350	0.93	18.075	58.16
25.03	9437.270	0.350	0.89	18.205	55.97
31.03	9443.384	0.409	0.93	–	51.68

**Fig. 2.** A separation of the He I λ 10830 Å line profile from the blend

line can be separated into two components: a narrow component from the slowly-rotating G6 giant and a broad component from the rapidly-rotating active F9 giant.

The fact that the broad profile is formed on the active, hotter star is supported by the radial velocity curves, obtained from the He I line for both stars and from the Si I line. Fig. 3 shows the radial velocity curves for both components of the Capella sys-

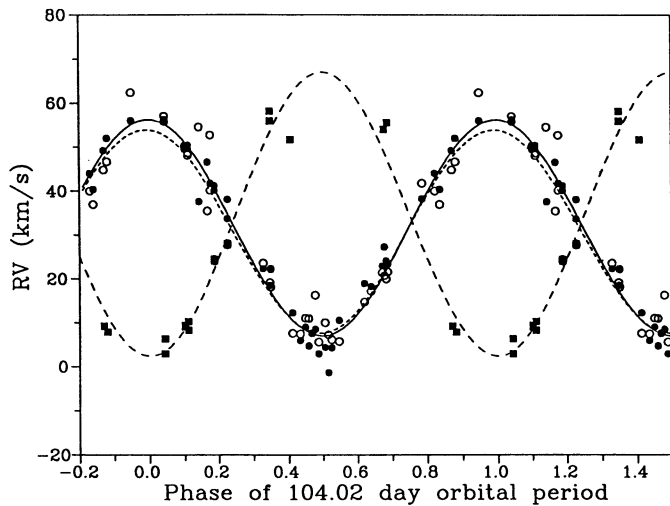


Fig. 3. Radial velocity curves for the Si I line (open circles), the narrow (filled circles) and the broad (black squares) component of the He I lines both for the primary, cooler and the secondary, hotter Capella's stars

tem. Two radial velocity curves obtained from the photospheric Si I $\lambda 10827 \text{ \AA}$ (open circles and the short-dashed line) and the narrow He I $\lambda 10830 \text{ \AA}$ (filled circles and a solid line) lines coincide rather well with the radial velocity curve of the cooler G6 primary star (Shen et al. 1985). The radial velocity measurements for the broad He I line (black squares and the long-dashed line) show good agreement with the radial velocity curve of the hotter F9 secondary. The radial velocities of the centre of gravity, determined from the He I line of the cooler primary (G6 III) and the active secondary (F9 III) components are close to each other: $\gamma = 31.62 \pm 0.24 \text{ km s}^{-1}$ and $\gamma = 32.19 \pm 0.84 \text{ km s}^{-1}$, respectively. There is also good agreement between these measurements and the radial velocity obtained here from the Si I line of the G6 giant ($\gamma = 30.77 \pm 0.96 \text{ km s}^{-1}$), and also with the radial velocity derived from the photospheric Si I line in 1985–1988, $\gamma = 31.67 \pm 0.52 \text{ km s}^{-1}$. There are some systematic differences between our new measurements and our previous radial velocity measurements derived from the He I line data in 1985–1988, $\gamma = 29.55 \pm 0.87 \text{ km s}^{-1}$, and also with the photospheric line radial velocity of Shen et al. 1985 ($\gamma = 29.48 \pm 0.07$). Such discrepancies could be due to insufficient length of our series of observations.

3.2. Variations of the equivalent width of the He I $\lambda 10830 \text{ \AA}$ line versus the orbital period

We found earlier that the equivalent width of the He I $\lambda 10830 \text{ \AA}$ line varies during the 104-day orbital period of Capella's binary, with the maximal He I absorption observed at phase 0.5 (Shcherbakov et al., 1990). Our subsequent observations demonstrate similar behaviour.

In Fig. 4, we plot the equivalent width values as a function of the phase of the 104-day orbital period for August 1985–April 1988 (open circles: Shcherbakov et al. 1990, 29 spectra), December 1989–March 1991 (open triangles: 16 spec-

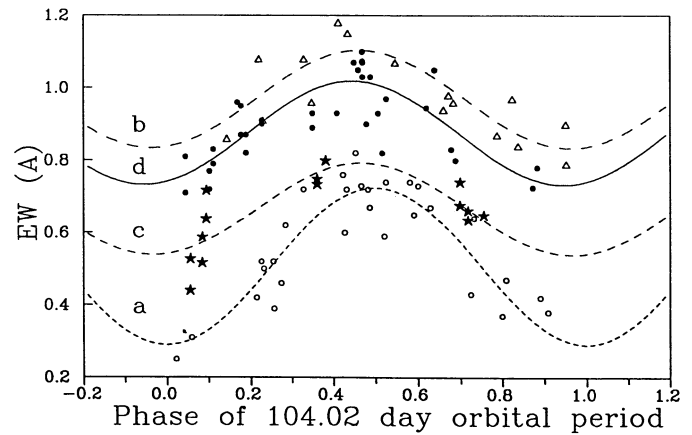


Fig. 4. Variations of the equivalent width of the He I line versus the phase of the 104-day orbital period during 10 years of our observations

tra), January–March 1993 (asterisks: 14 spectra) and September 1993–March 1994 (filled circles: 35 spectra). The EW-orbital phase dependence holds through the entire time interval of these observations, but the amplitude of the variations becomes significantly lower. If we present the set of equivalent width values for each of the time intervals considered as a sine law varying with the orbital phase, then the full amplitude of this sine curve $EW(\max) - EW(\min)$ is 0.27 in December 1989–March 1991 and 0.29 in September 1993–March 1994, but 0.43 in August 1985–April 1988. Thus, we observe smaller variation of amplitudes during the later time intervals, when the mean $EW(\text{He I})$ values are the higher, i.e. when the activity level of Capella is high.

Note that equivalent width variations with a period of 103.97 days are detected in the Fourier power spectrum, and the phase of these variations has been maintained through all our observations since 1980.

3.3. The long-term equivalent width variability of the He I $\lambda 10830 \text{ \AA}$ line)

To analyze the equivalent width of this helium line in more detail, we plotted the $EW(\text{He I})$ obtained by us in 1980 photographically together with our CCD data from 1985. A first look at the entire set of our observations in the near infrared helium line indicates that the equivalent width changed in quite a complicated way. However, a standard Fourier analysis of the temporal series since 1985 gives two periods: 2201.5 and 103.76 days. It is now possible to apply more refined periodogram analysis method.

Above, we presented the evidence for the existence of a long-term trend in the equivalent width of the He I line, as can be seen in Fig. 4. We proposed the presence of long-time cyclic equivalent width variations for the first time in 1983 (Katsova & Shcherbakov), based on an analysis of helium observations since 1968. However, the observational technique used did not permit reliable investigation of these variations. We will now analyse the data we have obtained since 1985 using a periodogram analysis method that compares the observed equivalent widths with a

model of the variability estimated by least-squares (LSQ) fitting of the observed data by trigonometric polynomials. The model period was interactively refined by Levenberg-Marquardt algorithm (Press & Teukolsky 1988). The result of this search for periods for the multi-periodic process is given in Fig. 5.

The final model after several iterations of the least-square fitting is

$$EW = EW_0 + A_0 t + A_1 \cos(2\pi t / P_1 + \phi_1) + A_2 \cos(2\pi t / P_2 + \phi_2),$$

where the parameters for the long-term variations are

$$EW_0 = 0.608$$

$$A_0 = 0.000122$$

$$P_1 = 2210 \text{ days}$$

$$A_1 = 0.212$$

$$\phi_1 = 1.84$$

and the parameters for the orbital variations are

$$A_2 = 0.25$$

$$P_2 = 103.9 \text{ days}$$

$$\phi_2 = -1.753.$$

This model is presented in Fig. 5 together with the observed EW(He I) values. The model gives an independent estimate (with no a priori assumptions) of the orbital period. The five-year period for the cyclic variations of the He I line equivalent width is derived from ten years of observational data, and represents a lower limit to the true duration of the activity cycle in Capella.

The model describes these observations with a good statistical determination. Formally, the sum of squares of residuals is

$$RSS \equiv \sum_{i=1}^{90} (EW_{obs} - EW_{model})^2 = 0.855 \text{ or } \sigma = \sqrt{\frac{RSS}{n(n-1)}} \approx$$

0.0103, where n is the number of independent measurements of the EW(He I) values. Amplitudes of the equivalent width variations discussed here are within $\pm 7\sigma$ for the orbital period variability and are of tens of σ for the long-term variations. The likelihood of the realization of this model is high enough, even in spite of the fact that it contains 6-7 independent parameters. It would be of interest to trace the long-term equivalent width variations found by us at the longer time interval. We tried to invoke results of our previous observations of Capella in the He I $\lambda 10830$ Å line in 1980–1982 (Katsova & Shcherbakov 1983), although they were obtained with an another technique (photomultiplier and high-sensitive infrachromatic film). Even with the lack of data in 1982–1985, we obtain that the phase of the orbital period is maintained through all the period 1980–1994, the equivalent width of the He I line varies with the period around 6 years, and the longer variations are possible as well.

4. Discussion

Investigations of Capella are of interest not only because it includes one or even two active late-type giants, but also because they form an RS CVn-type binary system. We have at our disposal a homogeneous dataset on the He I $\lambda 10830$ Å absorption line of Capella extending over as long as 10 years. We discovered the He I equivalent width variations with the phase of the 104-day orbital period in 1985–1988 (Shcherbakov et al., 1990); we

confirm here the presence of similar equivalent width variations in 1989–1994. The EW-orbital phase dependence thus holds throughout 1980–1994. Both the level of the absorption and the amplitude of the 104-day variations depend on the activity of the Capella system as a whole (see Fig. 4).

Other observational features that can help our understanding of the physical processes in the Capella system include the following facts:

1. The main He I $\lambda 10830$ Å absorption is located in the outer atmosphere, apparently the chromosphere, of the quiescent, cooler G6 giant. This conclusion follows from our radial velocity analysis (Fig. 3).
2. The activity of the Capella system is actually caused by activity on the hotter, F9 giant. We were able to extract directly the part of the He I absorption that forms in the outer atmosphere (apparently in the chromosphere) of this active star. The corresponding asymmetric He I $\lambda 10830$ Å line profiles are observed when the activity level of Capella is maximum. The depth of the He I $\lambda 10830$ Å absorption line observed for the F9 III star during the maximum of its activity cycle is no less than 10%. Since the near infrared continuum of the G6 III star is a factor of 3 brighter than that of the F9 III star, we conclude that $fA = 0.4$, where f is the depth of the He I $\lambda 10830$ Å absorption line from the F9 giant and A is the total area of active regions in units of the stellar disk area. If the depth in the centre of the broad absorption line is 100% ($f = 1$), then about 40% of the visible disk of the F9 giant should be occupied by active regions (their solar analogues are plages, which are bright in the H_α line and very dark in the He I $\lambda 10830$ Å line). This active region area is very large compared to that on the Sun, and the stellar plages are distributed rather homogeneously over the F9 giant surface, as follows from the rotational modulation of the EW(He I) for the F9 star. Additional analysis gives the EW(He I) values for the F9 giant ≤ 0.17 Å, which varies with the period of the axial rotation of the F9 giant of about 8 days. However, this rotational modulation is not very pronounced, possibly due to a more or less homogeneous distribution of active regions over the F9 giant surface; these active regions are revealed by their UV, EUV, and soft X-ray emission (Ayres 1988, Dupree et al. 1993). We will discuss this in a future paper. The solar-type activity of the cooler, G6 giant primary is significantly weaker than that of the hotter F9 giant, and is consistent with the analysis of the UV-lines of Capella by Ayres (1988).
3. The total He I absorption undergoes long-term variations that may be due to the existence of an activity cycle with a period of 6 years on the F9 giant.

The temporal behaviour of the He I $\lambda 10830$ Å absorption line is quite complicated, and can not be explained in the framework of a simple model. We proposed earlier that the He I line is formed on the active F9 giant (Katsova & Shcherbakov 1983). Although the intensity of the near infrared continuum of the active component is several times lower than that of the G6 giant, we hoped to find this line on the F9 giant. However, further He I

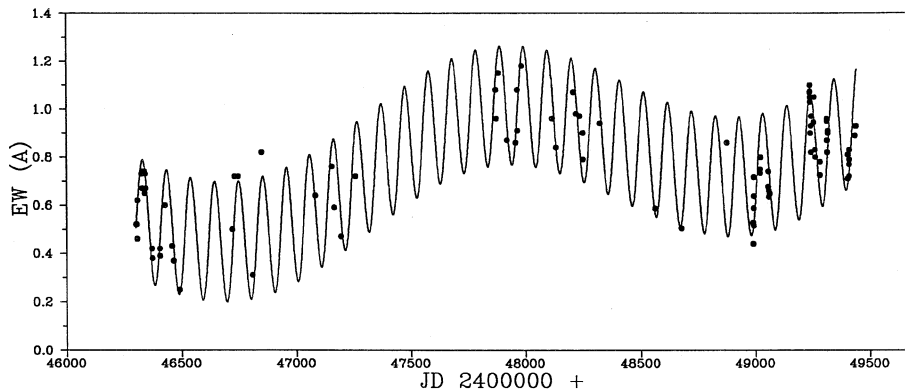


Fig. 5. Fit of periodicity model to the observations of the He I line obtained in 1985-1994 with two periods of 2210 days and 103.9 days

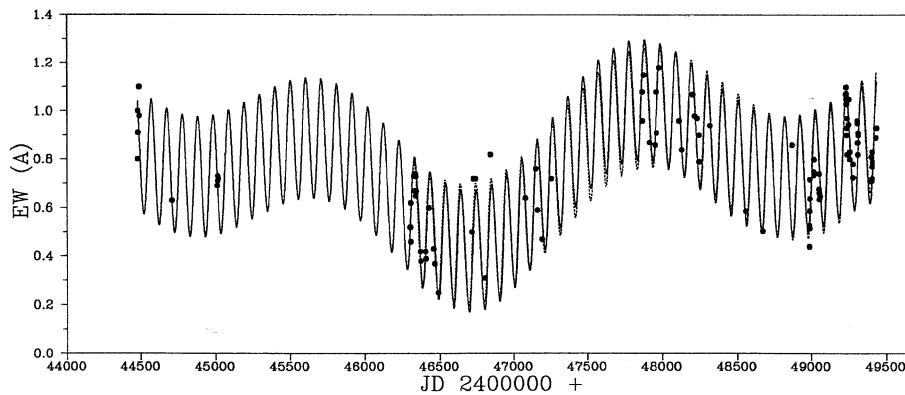


Fig. 6. Fit of periodicity model to the observations of the He I line obtained in 1980-1994 with two periods of 2210 days and 103.9 days (dashed line) and with three periods of 3928 days, 1964 days, and 103.7 days (solid line)

observations showed that the main He I absorption occurs in the outer atmosphere of the G6 giant, as follows both from the radial velocity analysis and from the dependence of the He I equivalent width on the orbital phase. Therefore, we were forced to consider a more complicated model of Capella, including the effects of the stellar wind from the active component on the outer atmosphere of the quiescent giant (Katsova 1992, 1995).

The observations presented here can be understood in the framework of the following, more developed model. Let us suppose that there are one or several large-scale coronal structures on the F9 giant filled by hot plasma at a temperature $T \leq 10^7$ K, which are sources of an enhanced stellar wind. Some flow arises near the Lagrangian point L_1 as a result of the joint effect of these streams from isolated regions on the F9 giant. The interaction of this flow with the corona of the quiescent G6 giant or its stellar wind leads to formation of a shock wave. The gas behind the shock front should be observable at soft X-ray and EUV wavelengths even against the background radiation of the F9 giant in these spectral ranges. More likely, the source of this radiation should be best observable at orbital phases around 0.5. There is reason to suppose that the EUV source, observed by Dupree & Brickhouse (1995) is associated with radiation formed behind the proposed shock wave front. Note that according to the EUVE data, the Fe XX–Fe XXIII line fluxes show variations with orbital phase similar to those for EW(He I) (see Fig. 2 in Dupree & Brickhouse, 1995).

Thus, this schematic picture allows us to explain all our observational data in a natural way. The main absorption in the 10830 Å line arises in the chromospheric region of the quiescent

star, which is located beneath the shock front and is revealed by its EUV radiation. This region is most clearly observable at orbital phases around 0.5. The strength and location of the shock wave are mainly determined by a particle flow of the wind formed on the isolated region of the active F9 giant. When this flow varies, this is reflected in the main He I absorption.

Note that if the above proposed model with an intensive magnetized stellar wind from the F9 giant is valid, then the age of the Capella system should not exceed 10^8 years. Although this estimate of the age of Capella is several times smaller than the age estimate based on evolutionary tracks, it does not contradict the evolutionary states of these stars: the hotter component is crossing the Hertzsprung gap and now very close to the time when its central hydrogen will be exhausted, and the cooler giant has already undergone helium ignition. More details and a discussion of the evolutionary status of Capella are discussed by Katsova (1997).

Acknowledgements. We would like to thank Dr. A.K. Dupree for presenting us with the EUVE data for Capella prior to their publications, Prof. M.A. Livshits for helpful discussions, and the referee, Prof. C. de Jager, for useful comments. The research described in this publication was made possible in part by Grants R2Q000 and U1C000 from the International Science Foundation and by Grant A-05-067 from the ESO C&EE Programme. The work by MMK is supported in the framework of the State Scientific-Technical Program of Russia “Astronomy.”

Appendix

In addition to the above presented temporal behaviour of the equivalent width of the He I $\lambda 10830$ Å line (see 3.3), we give also

another model, that also describes the full set of our observations since 1980:

$$EW(t) = EW_0 + A_1 \cos(2\pi t/P_1 + \phi_1) + A_2 \cos(2\pi t/P_2 + \phi_2) + A_3 \cos(2\pi t/P_3 + \phi_3),$$

where the mean value of the equivalent width EW_0 is 0.765 and the parameters of the long-term variations are

$$A_1 = 0.174$$

$$P_1 = 3928 \text{ days}$$

$$\phi_1 = -0.035,$$

and

$$A_2 = 0.187$$

$$P_2 = 3928/2 = 1964 \text{ days}$$

$$\phi_2 = -2.107,$$

and the parameters of the orbital variations are

$$A_3 = 0.25$$

$$P_3 = 103.70 \text{ days}$$

$$\phi_3 = 0.673.$$

The longer period is $P_1 \approx 10.8$ years, while the period P_2 can be considered both a harmonics of the period P_1 . The long-term linear trend, revealed in 3.3 in data for 1985-1994, is apparently representative of long-term variations with the period around 11 years or even of the longer one. The comparison of this solution with that presented in 3.3 (dashed line in Fig. 6) shows a good agreement of both models at overlapping time intervals, and indicates that the phase of the orbital period has been maintained through 14 years.

Thus, this analysis as well as the one given in 3.3 shows that the equivalent width of the He I $\lambda 10830$ Å line in Capella varies with the period of 5–6 years, but the longer period is possible as well.

References

Ayres T.R., 1988, ApJ 331, 467

Ayres T.R., Linsky J.L., 1980, ApJ 241, 279

Beresin V.Yu., Zuev A.G., Kiryan G.V., Rybakov M.I., Hvilivitsky A.G., Ilyin I.V., Petrov P.P., Savanov I.S., Shcherbakov A.G., 1991, Pis'ma Astron.Zh. 17, 953 (in russian)= Sov.Astron.Lett. 17, No 5
Dupree A.K., Brickhouse N.S., Doschek G.A., Green J.C., Raymond J.C., 1993, ApJ 418, L41

Dupree A.K., Brickhouse N.S. 1995 in: Stellar Surface Structure /Ed.K. Strassmeier. Proc.IAU Symp.176, Vienna, Oct.1995. Poster Paper p. 184

Fekel F.C., Moffett T.J., Henry G.W., 1986, ApJS 60, 551

Huovelin J., Poutanen M., Tuominen I., 1986, Helsinki Univ.of Techn. Radio Lab. Report S166, 18

Ilyin I.V., 1995, Acquisition, archiving and analysis (3A) software package and User's Manual, Observatory, University of Helsinki

Katsova M.M., 1992 in: Surface Inhomogeneities on Late-Type Stars eds. P.B.Byrne, D.J.Mullan, Lecture Notes in Physics, Springer, v. 397 p. 220

Katsova M.M., 1995 in: Stellar Surface Structure ed. K.Strassmeier, Proc.IAU Symp.176, Vienna, Oct.1995. Poster Paper p. 187

Katsova M.M., 1997 in: Ap SpSc, in press

Katsova M.M., Livshits M.A., 1978, Sov.Astron. 22, 208

Katsova M.M., Shcherbakov A.G., 1983, Sov. Astron. 27, 153

Linsky J.L., Wood B.E., Judge P., Andrusis C., Ayres T.R., 1995, ApJ 442, 381

Press W.H., Teukolsky S.A., 1988, Computers in Physics 2, 77

Shcherbakov V.A., 1994, Licensed Package "CCD Image Fitting", Crimean Astrophysical Observatory, Crimea, Ukraine

Shcherbakov A.G., Tuominen I., Jetsu L., Katsova M.M., Poutanen M., 1990, A&A 235, 205

Shen L.-Z., Beavers W.I., Eitter J.J., Salzer J.J., 1985 AJ 90, 1503

Wood B.E., Ayres T.R., 1995 ApJ, 443, 329

Zirin H., 1976 ApJ 208, 414

This article was processed by the author using Springer-Verlag L^AT_EX A&A style file L-AA version 3